

Supplementary Information for:

Impacts of Climate Change Induced Sea Level Rise, Flow Increase and Vegetation Encroachment on Flood Hazard in the Biobío River, Chile

Gerhard Schoener ^{1*}, Enrique Muñoz ^{2,3}, José Luis Arumí ^{4,5} and Mark C. Stone ⁶

¹ Southern Sandoval County Arroyo Flood Control Authority, 1041 Commercial Dr SE, Rio Rancho, NM 87124, USA

² Department of Civil Engineering, Universidad Católica de la Santísima Concepción, Concepción 4030000, Chile; emunozo@ucsc.cl

³ Centro de Investigación en Biodiversidad y Ambientes Sustentables (CIBAS), Universidad Católica de la Santísima Concepción, Concepción 4030000, Chile

⁴ Water Resources Department, Faculty of Agricultural Engineering, Universidad de Concepción, Chillan 3812120, Chile; jarumi@udec.cl

⁵ Water Research Center for Agricultural and Mining (CRHIAM), Universidad de Concepción, Concepción 4090541, Chile

⁶ Department of Civil, Construction and Environmental Engineering, University of New Mexico, Albuquerque, NM 87131, USA; stone@unm.edu

* Correspondence: gschoener@sscafca.com

Table S1: Calculated recurrence intervals and associated peak flows and 95% confidence limits for the lower Biobío River based on annual maximum time series using the method outlined in USGS Bulletin 17.

Chance Exceedance %	Recurrence Interval y	Flow m ³ s ⁻¹	Confidence limits	
			0.05 m ³ s ⁻¹	0.95 m ³ s ⁻¹
0.2	500	18,959	32,610	14,164
0.5	200	17,162	26,697	13,429
1	100	15,715	22,784	12,722
2	50	14,184	19,267	11,838
5	20	12,009	15,074	10,304
10	10	10,222	12,198	8827
20	5	8265	9608	7127
50	2	5207	6092	4425
80	1.25	3037	3619	2331
90	1.11	2219	2723	1462
95	1.05	1684	2159	922
99	1.01	961	1411	328

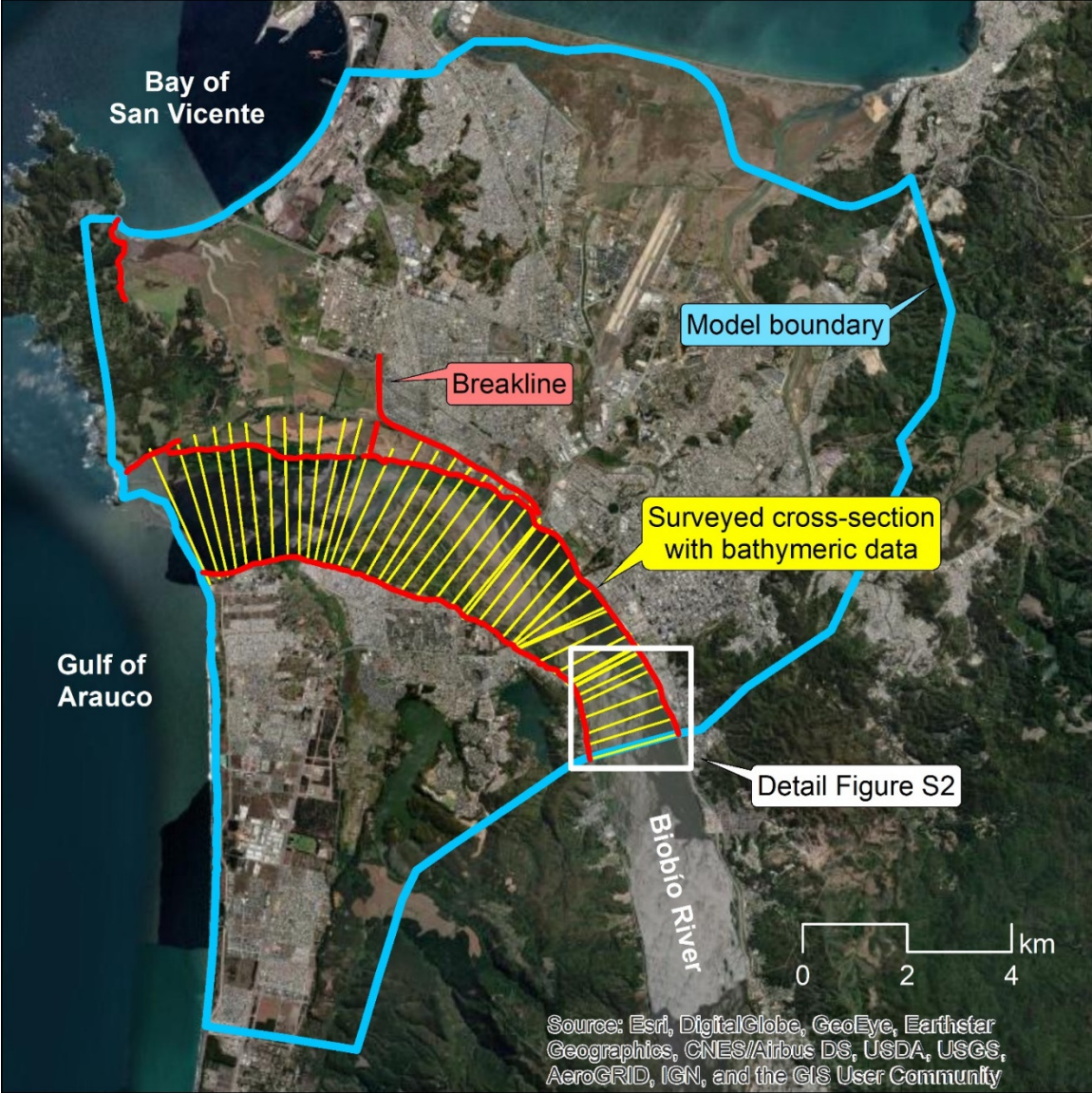


Figure S1: Map of the study area showing the boundary of the hydrodynamic model (blue), breaklines used to refine the computational mesh (red), and locations of surveyed cross-sections (yellow).

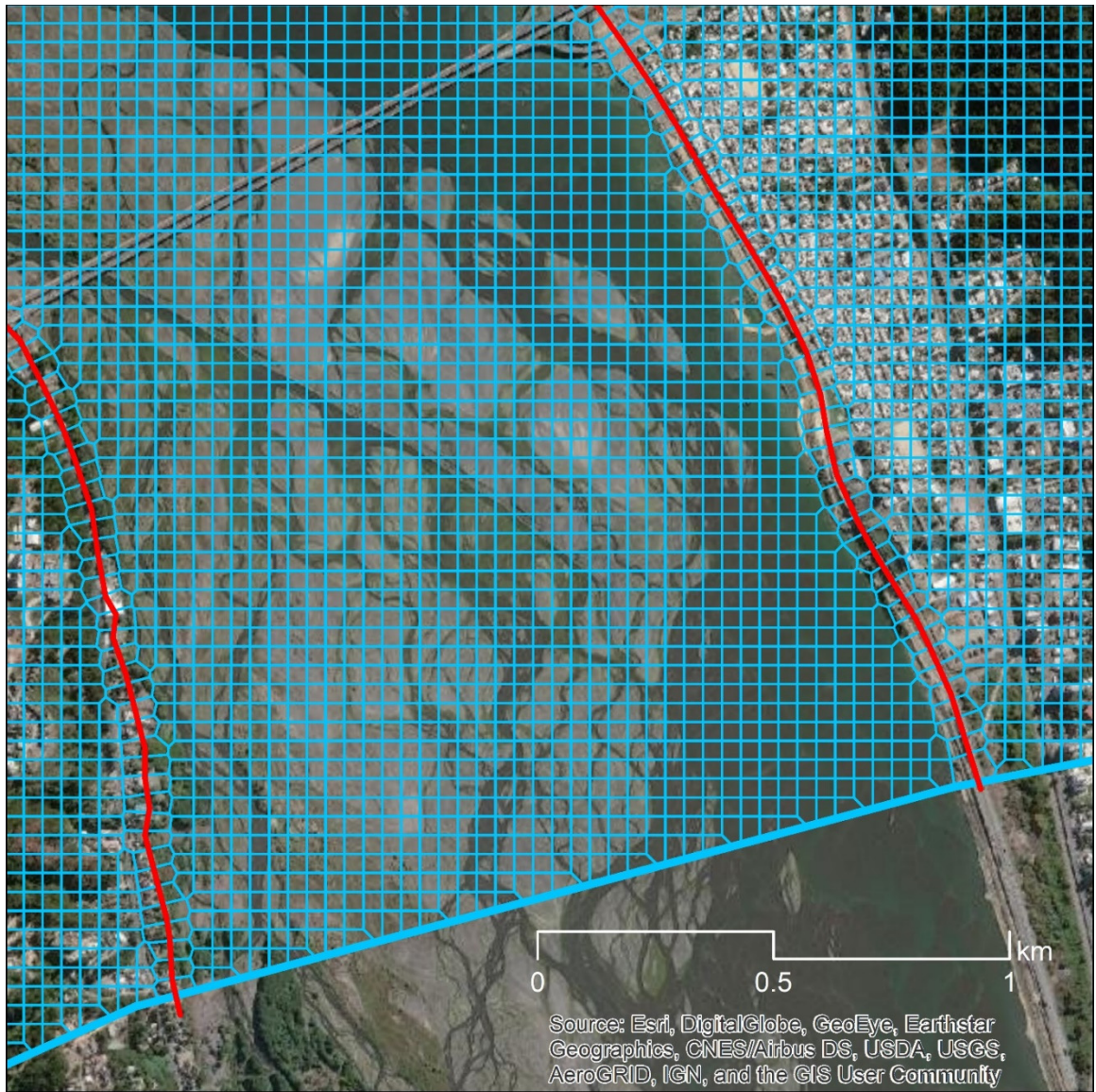


Figure S2: Detailed view of a portion of the computational mesh (blue) and refinement regions along the banks of the Biobío River (red).

Table S2: Manning's n -values for different land use types.

Land use	n -value	Land use	n -value
barren land	0.027	shrubland	0.120
dunes	0.030	forest	0.140
river channel	0.032	dense riparian forest	0.160
pasture/field	0.040	urban area, low density	0.080
wetland	0.050	urban area, medium density	0.120
scrubland	0.070	urban area, high density	0.160

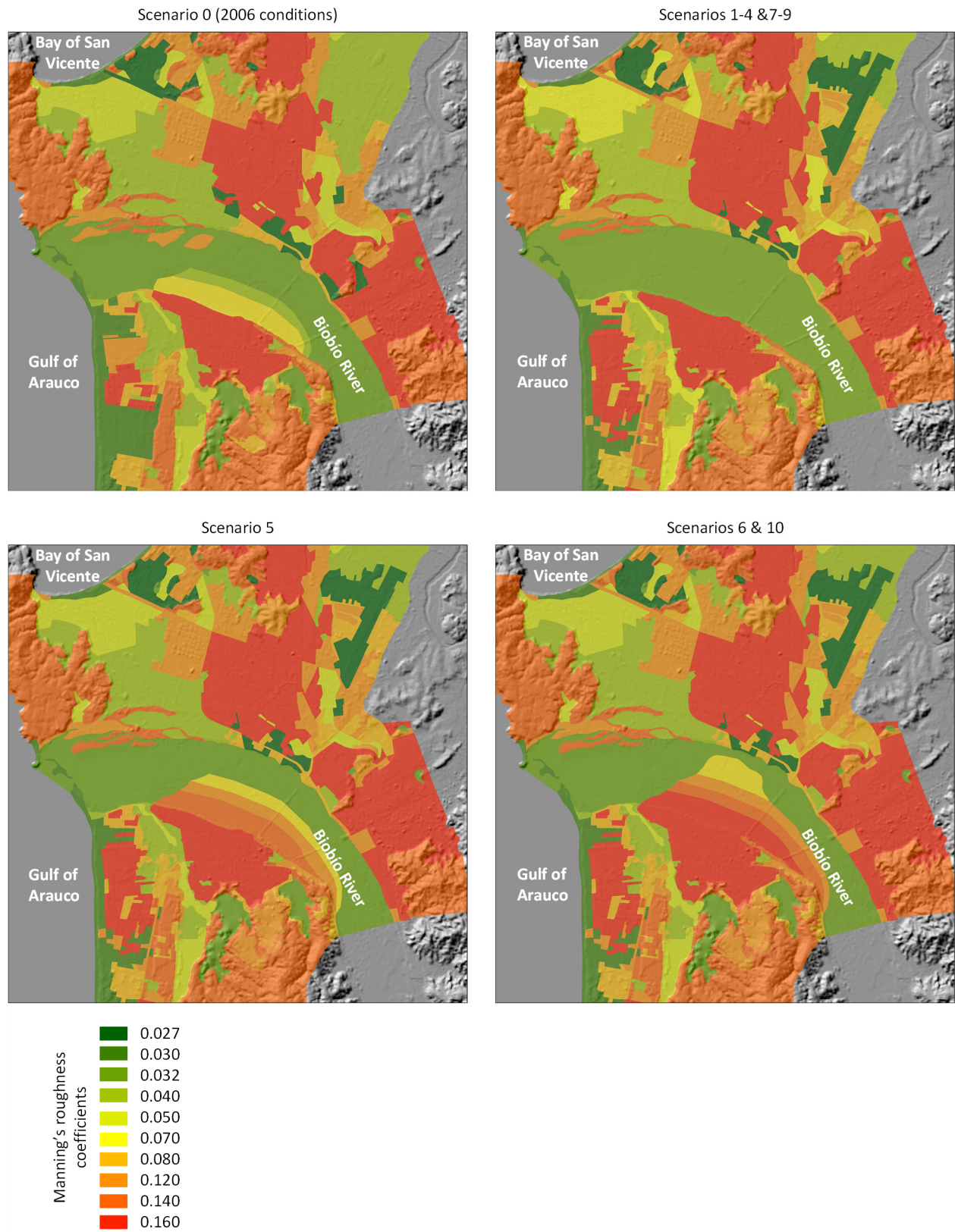


Figure S3: Manning's n -values for different model scenarios.



Figure S4: Overview map (top) showing locations where modeled and observed flood extent for the 2006 flood were compared, and comparison at location 1 (bottom; see red line for comparison; image source: Didier Rousset Buy).



Figure S5: Comparison of modeled (left) and observed flood extents (right) at locations 2, 3 and 4 (see red line for comparison; image source: Didier Rousset Buy).

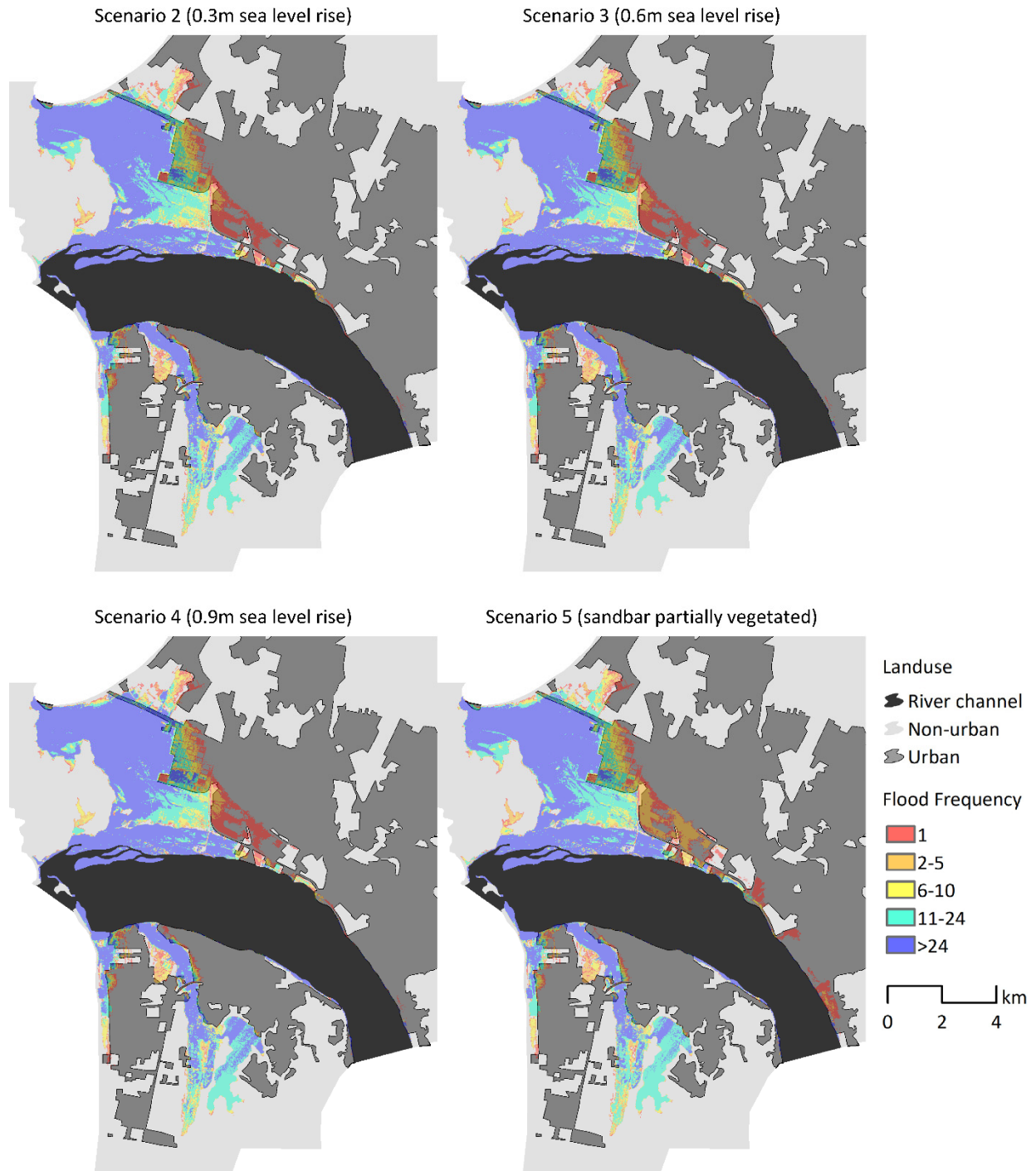


Figure S6: Maps showing frequency of flooding in the study area based on 32 flood events for scenarios 2-5. The river channel is indicated with black shading; areas urbanized in 2022 are indicated with a darker shade of grey.

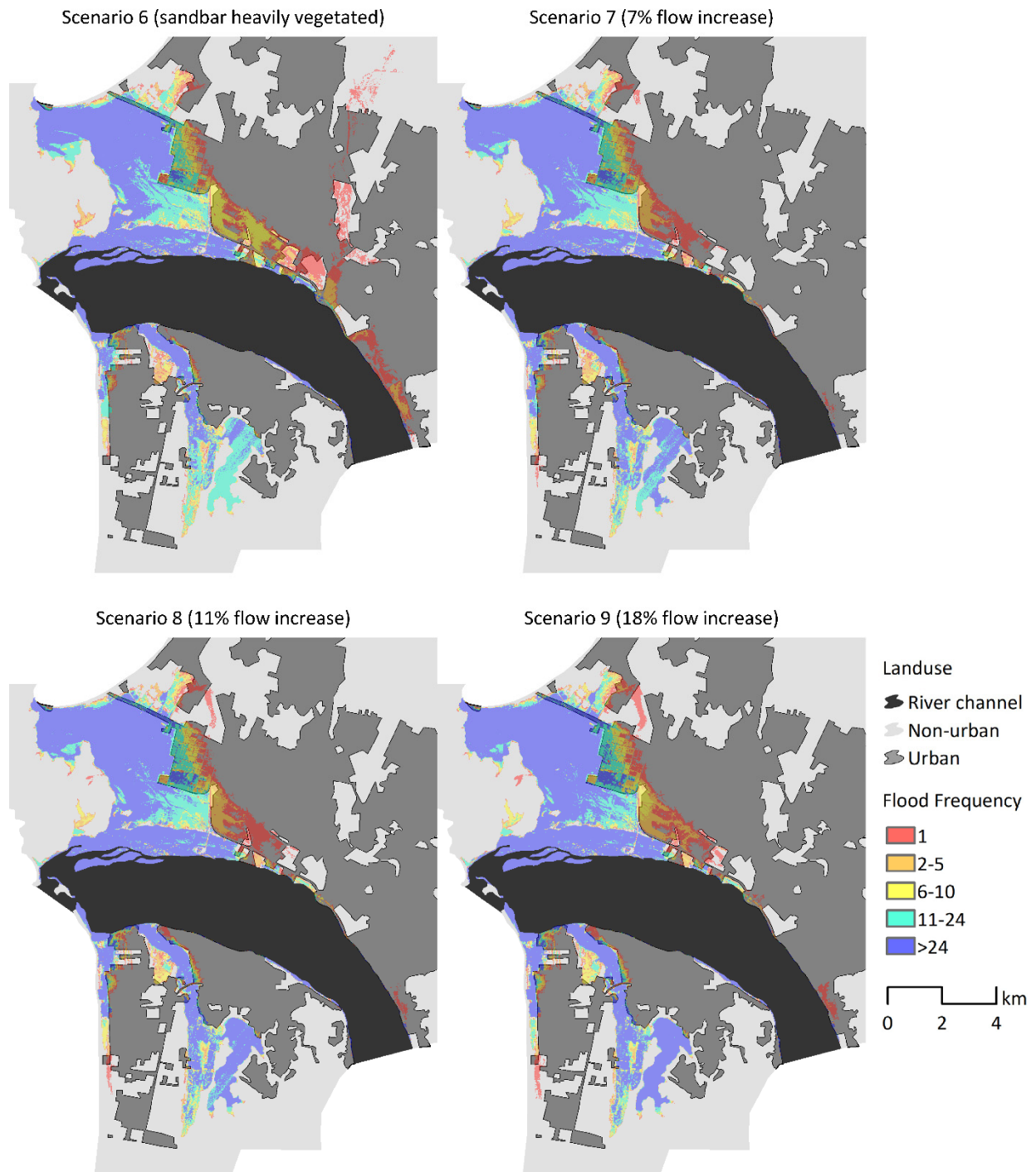


Figure S7: Maps showing frequency of flooding in the study area based on 32 flood events for scenarios 6-9. The river channel is indicated with black shading; areas urbanized in 2022 are indicated with a darker shade of grey.



July 2005



March 2009



March 2013



March 2022

Figure S8: Photos showing the confluence of the Ñuble and Itata Rivers (Latitude: -36.642239° , Longitude: -72.466197°) in central Chile in 2006, 2009, 2013 and 2022 (image source: José Luis Arumí).